IOP Conference Series: Earth and Environmental Science

PAPER • OPEN ACCESS

Estimation of possible climate change impact on methane hydrate in the Arctic Ocean

Estimation of possible climate change impact on methane hydrate in the Arctic Ocean

V V Malakhova[1], E N Golubeva[1,2], A V Eliseev[3,4], and G A Platov[1,2]

[1]Institute of Computational Mathematics and Mathematical Geophysics of SB RAS, Novosibirsk, Russia
[2]Novosibirsk State University, Novosibirsk, Russia
[3]Lomonosov Moscow State University, Moscow, Russia
[4]A.M. Obukhov Institute of Atmospheric Physics, Russian Academy of Sciences, Moscow, Russia

Abstract. We study the potential impact of a possible warming in the Arctic Ocean in the 21st century on the methane hydrates stability zone. In order to assess the space-time variability of the ocean bottom temperature, we employ a regional version of a coupled ice-ocean model that has been developed at the Institute of Computational Mathematics and Mathematical Geophysics, Siberian Brunch of the Russian Academy of Sciences. This study is based on a combination of the coupled ocean-ice model and a one-dimensional thermal diffusion sediment model. As an atmospheric forcing, some results obtained with CMIP5 climate models simulated with the RCP8.5 scenario (from 2006-2100) are used. We have found that warm North Atlantic water will have a major influence on the Arctic gas hydrates. In such regions as the Barents Sea, the West Svalbard continental margin, and the continental shelf of Norway methane hydrates may exist in shallow waters, where the strongest warming occurs. For this reason, these regions are most vulnerable to releasing methane into the ocean and the atmosphere when the sea water temperature is increased by approximately 2-3 °C. According to our estimates, the seafloor water warming in these areas during the next 100 years may lead to a shift in the upper boundary of the gas hydrates stability zone by 10-110 m.

1. Introduction

Gas hydrates are ice-like crystalline compounds of water and gas, basically, methane that occupy the porous space of marine sediments. Methane hydrates are formed at sufficiently high pressures and low temperature conditions provided that a sufficiently large volume of methane is available [1]. The gas hydrate stability zone (GHSZ) is a part of the Earth's lithosphere and hydrosphere where the thermodynamic conditions correspond to the gas hydrate steady state.

The methane hydrates were discovered in the seafloor deep water sediments (exceeding 300 m) along the continental margins and within the permafrost areas, both continental and relic subsea permafrost, particularly in the Arctic regions. Conditions for the formation of methane hydrates are found in the Arctic Ocean [2]. The Arctic marine sediments preserve large quantities of methane in gas hydrates, whose stock is estimated as 100-9000 GtC [2, 3, 4]. The assessments of methane in subsea permafrost-associated gas hydrates are in the range from 2 to 1400 GtC [2]. The shallow gas hydrates of the Arctic regions might dissociate and release large quantities of methane if oceanic water is warmed.

The last decades are characterized by significant climate changes, most pronounced in the polar latitudes of the Northern Hemisphere [5]. The most striking among them is a statistically significant positive linear trend of the average annual air temperature in 1936-2007, reduction in the sea-ice area in the summer period and the volume of the multi-year ice of the Arctic Ocean, degradation of the underwater permafrost, and the destruction of the shores of the Arctic seas [6].

Warming of the ocean bottom water and thawing of the subsea permafrost can destabilize hydrate deposits and lead to methane release. The growing interest in studying this atmosphere greenhouse gas is due to a higher radiation activity of methane as compared to carbon dioxide. Methane that migrates to the seafloor after dissociation may be released into the water at shallow water depths and into the atmosphere. The loss of sea ice is likely to increase in the 21st century, and, therefore, sea-air exchange of methane will also be enhanced [7]. Release of methane from melting hydrates and oxidation to CO_2 could enhance the ocean acidification and oxygen depletion in the water column [3].

By now the measurement data have revealed an increase in the methane emission into the atmosphere of the Arctic [7-11], which can occur as a result of the submarine gas hydrates dissociating [8, 7, 9] and the subsea permafrost thawing [10, 11].

In the shallow Arctic shelf with a water depth not exceeding 100 m, the existence of gas hydrate deposits is possible if the subsea permafrost is present in sediments [12, 13]. In study [14], the sensitivity of the permafrost-related hydrate reservoirs to warming up to the end of the 21st century was investigated. According to the model results, if the warming will continue until the end of the 21st century, the permafrost-related gas hydrates will respond very slowly to changes in the bottom water temperature [14]. In paper [13], simulations with a model for a thermal state of the submarine permafrost forced with the data from the ice core reconstructions are performed, and it is shown that the time scale of heat propagation is 10-20 kyr. The present-day methane emissions [11] can be associated with the processes of much longer time scales [15], for example, associated with the thermokarst processes in the Holocene [16].

In [7], it was concluded that the release of methane from the seas of the Arctic Ocean is only slightly smaller than that from the continental Arctic, with 2/3 of the marine emissions concentrated in the seas of the western part of the Arctic. The maximum anomalies of methane concentration were observed in November-December over the sea surface along the coasts of Norway, Novaya Zemlya, Svalbard, and other regions of the Arctic. A significant part of the methane emission from the seas occurs in the regions with a sea depth in the range from 100 to 300 m. The GHSZ in these areas begins at sea depths of 250-300 m, and with rising of the bottom water temperature at these depths methane hydrates can be prone to dissociation. The estimates of the sensitivity of the GHSZ to the warming of the bottom water temperature in the Arctic Ocean obtained earlier on the basis of simulation [17] are confirmed by the conclusions for the western Arctic seas [7]. Study [17] has revealed that reduction of the methane hydrate stability zone occurs in the Arctic Ocean between 250 and 400 m water depths within the upper 70 m of sediments in the Atlantic inflow area within 10-20 years.

The goal of this study is to analyze the sensitivity of the marine sediment GHSZ of shallow and mid-depth regions of the Arctic Ocean to the climate changes by the end of the 21st century with a scenario of the anthropogenic impact on the climate system. The present study combines the seafloor temperature increase projections with calculations of the GHSZ thickness changes over time. The scenario RCP8.5 is used, since it predicts the strongest warming by the end of the 21st century.

We use a set of interacting numerical models to study the effect of climate changes on the ice cover, the thermohaline structure of the Arctic Ocean, and the gas hydrate stability zone. The set of the numerical models includes: a regional version of the coupled ice-ocean model (SibCIOM), which was developed at the Institute of Computational Mathematics and Mathematical Geophysics, Siberian Brunch of the Russian Academy of Sciences [18, 19]; a model of the thermophysical processes in sediments [13, 17], and the methane hydrate stability condition as reported in [20].

To obtain the ocean and sea ice surface currents, the NCEP / NCAR atmosphere reanalysis data [21] were used for 1948-2006 and the results of calculations of the climate system models participating in the CMIP5 project [22] with the scenario RCP8.5 for 2006-2100.

2. Data and methods

2.1. *The ocean model*

The SibCIOM ocean model [18, 19] is based on the conservation laws for heat, salt, and momentum formulated under hydrostatic, Boussinesque, and "rigid lid" approximations. After the separation of the momentum equations into the external and internal modes, the barotropic equations are expressed in terms of a stream function. When integrating over time, a hybrid explicit-implicit scheme and splitting to the physical processes and spatial coordinates are used. The QUICKEST scheme is employed to approximate advection, while the multidimensional extension uses the COSMIS approach [23]. The vertical adjustment is considered as a mixed layer parameterization based on the Richardson number [24]. The ocean circulation model was coupled with the CICE v3 model of the thermodynamics of elastic viscous-plastic ice [25] and multi-category sea ice thermodynamics [26]. The sea ice advection utilizes a semi-Lagrangian scheme [27].

For the current study, the simulation domain included the Arctic and the Atlantic Ocean north of 20°S. The grid resolution for the North Atlantic was chosen to be 0.5°x 0.5°. At 65°N, the North Atlantic spherical coordinate grid is merged with the displaced poles of the Arctic grid. In the Arctic, an average grid spacing is about 18 km. The model version used here has 38 unevenly spaced vertical levels with a maximum resolution of 5 m in the upper 20-meter layer. No-slip boundary conditions at the solid boundaries are used. The specified mass transports at open boundaries and river inflows are compensated by transports through the outflow boundary at 20° S. At the initial stage the model is forced with the NCEP/NCAR reanalysis data [21]. The initial distribution of the temperature and salinity fields corresponds to the climatic data of the Polar Science Center Hydrographic Climatology [28] for the winter period.

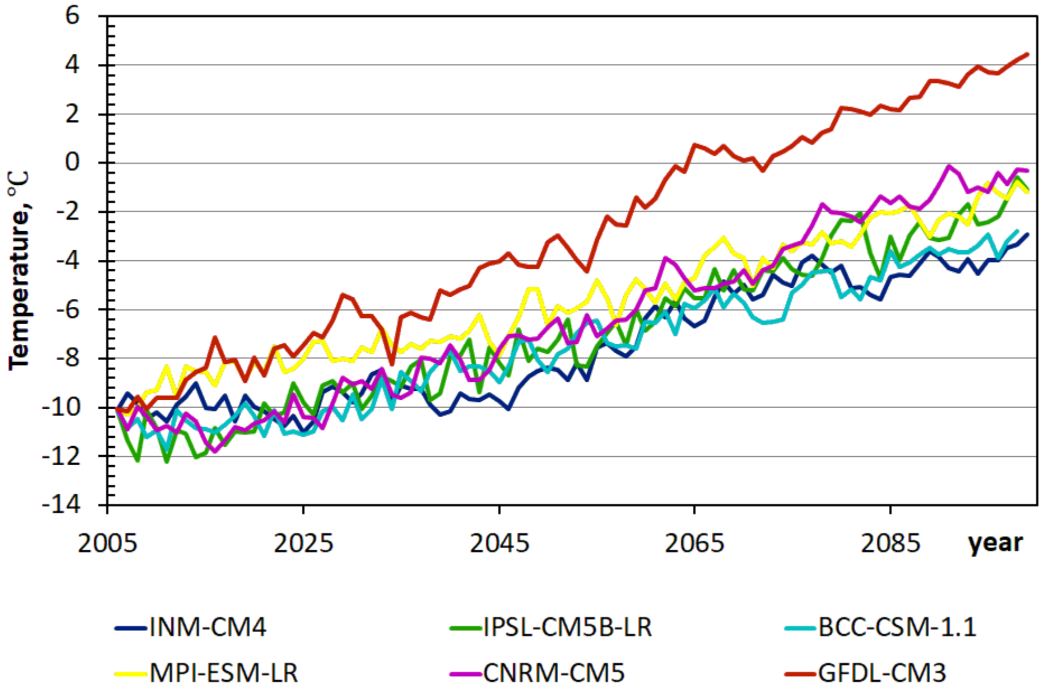

Figure 1. Air temperature predictions based on six CMIP5 models under RCP8.5 scenario from 2006 to 2100 in the Arctic north of 65 °N.

2.2. Future climate conditions

A preliminary analysis of the CMIP5 model data archives has shown that they can be divided into several groups which differ from each other by the climate in the early 21st century, and also by the warming in the Arctic region [29] (see Figure 1). As a consequence, six models were selected for further analysis, each as a representative for one of the groups:

1) INM-CM4: the model characterized by the least warming in the Arctic in the 21st century.
2) BCC-CSM-1.1: the model is also characterized by a relatively small warming in the Arctic. However, this model reveals a significant increase in the temperature of the lower atmosphere in the Norwegian Sea and in the northwestern part of the Barents Sea.
3) IPSL-CM5B-LR: the model belonging to a group of models with moderate warming above the Arctic Ocean in the 21st century accompanied by larger warming near Novaya Zemlya.
4) MPI-ESM-LR: the model also belonging to a group of models with moderate warming above the Arctic Ocean. However, unlike the IPSL-CM5B-LR model, the warming is relatively homogeneous over space in the whole Arctic water area.
5) CNRM-CM5: the model is characterized by moderate warming above the Arctic Ocean, and, like BCC-CSM-1.1, an increase in the temperature of the lower atmosphere in the Arctic region is greatest in the Norwegian Sea and in the northwestern part of the Barents Sea.
6) GFDL-CM3: the model with a very strong warming in the Arctic.

The state of the ocean and sea ice obtained as a result of the first stage of the simulation (from 1948 to 2006) based on the SibCIOM model was used as initial fields for the modeling of the future state of the ice-ocean and bottom sediments up to the end of the 21st century under the scenario of the anthropogenic impact on the climate system (RCP 8.5). When carrying out the experiments, anomalies of the atmospheric forcing were set for 2006-2100 in the form $Y_M(t)$-$Y_M(2006)$+$Y_R(2006)$, where $Y_M(t)$ is an atmospheric variable calculated from the CMIP5 model data (t indicates the time instant), and Y_R is the corresponding variable calculated from the NCEP / NCAR data. This method of specifying the atmospheric forcing for the oceanic model provides the absence of a jump in the transition from the reanalysis data to the data calculated based on the CMIP5 models. The expression $Y_M(t)$-$Y_M(2006)$+$Y_R(2006)$ was calculated taking into account the annual variation of the atmospheric variables in 2006.

2.3. Gas hydrate stability zone simulation

To evaluate the temperature fields in the ocean sediments, we use a model for the thermal state of the subsea sediments [17]. With this model we solve a one–dimensional heat diffusion equation in a sediment column subject to a prescribed temperature at the sediment–ocean interface and a prescribed heat flux at the lower boundary. The model has a total height of 1000 m and a vertical grid cell height of 0.5 m. We set an average sediment thermal conductivity as 1.5 W/m·K [30]. A more detailed description of the numerical model is available in [17].

We made use of the bottom water temperatures of the past (1948-2005) and future bottom water temperatures (2006-2100) as the upper boundary condition or the one-dimensional thermal diffusion sediment model. In this study, the geothermal gradients were calculated based on the heat flux reconstruction [31] with values of 20-120 mWm^{-2}. The initial temperature profile in the sediment is in equilibrium with the seabed bottom water temperature data adopted for 1948 [28] and the geothermal flux [31]. In the period from 1948 to 2100 we simulate the transient heat exchange between the bottom water and the ocean sediment. In this study, we do not consider a potential effect of the hydrate zone on the temperature field evolution.

For a time step equal to one month, the GHSZ thickness for each sediment column was determined by using the pressure-temperature equilibrium condition of the methane hydrate system. In this case we used the model of heat transport in sediment, the bottom water temperature, and the geothermal heat flux data. The methane hydrate stability condition is based on the general regression reported in [20]. The GHSZ was simulated as a part of the sediment column in which the pressure exceeded the dissociation pressure. The water depths in the numerical domain corresponded to the vertical resolution from the SibCIOM model and further converted to pressure. In order to simulate the presence of a sulfate reduction zone, we set the top of the sediment column (7 m) to be free from hydrates [32]. However, the presence of methane in the pore space is not provided, since there is no detailed information on the distribution and concentration of methane hydrate in the sediment. Therefore, the methane hydrate stability condition is necessary but not sufficient for the presence of gas hydrate.

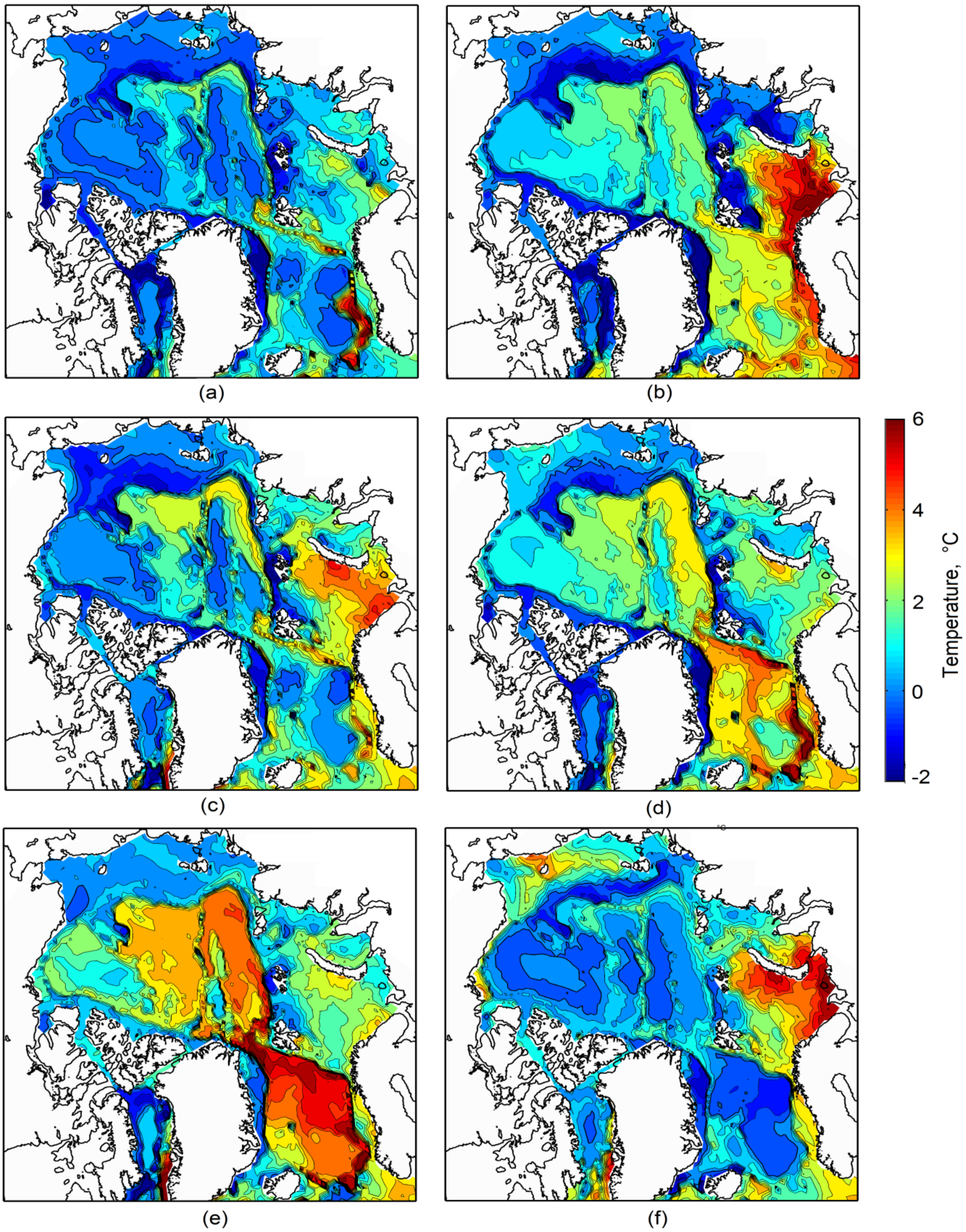

Figure 2. Bottom water temperature changes (2091–2100 minus 2006–2010) obtained in a numerical experiment with atmospheric forcing using models with the RCP 8.5 scenario: (a) INM-CM4, (b) BCC-CSM-1.1, (c) IPSL-CM5B-LR, (d) MPI-ESM-LR, (e) CNRM-CM5, (f) GFDL-CM3. Bold black contour indicates 0-°C isotherm.

The initial GHSZ thickness is determined by the hydrostatic pressure distribution and the initial temperature in the sediment column. The transient evolution of the methane hydrate stability zone for each sediment column with a 1-month time step was calculated in the period from 1948 to 2005 and then from 2006 to 2100 according to the sediment temperature.

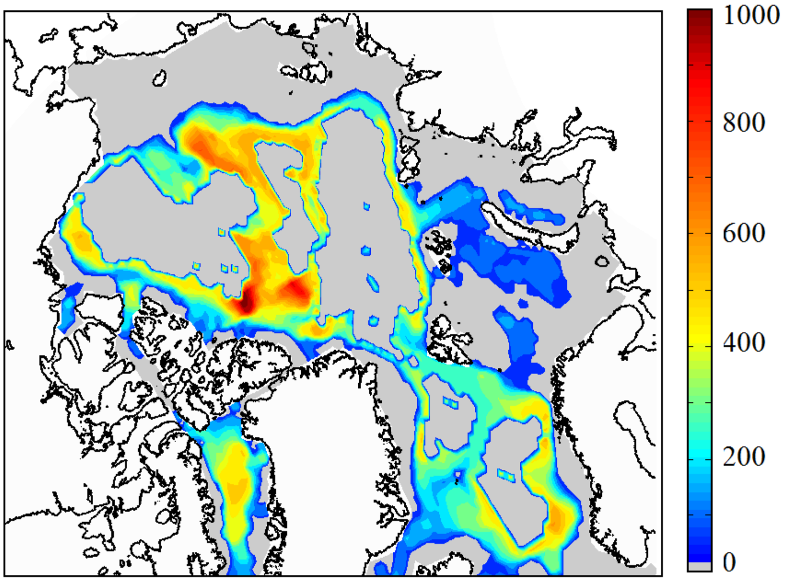

Figure 3. Gas hydrate stability zone (in meters) for 2006 over the Arctic region simulated in this study.

3. Results

Analyzing the predicted future state of the ocean obtained in the course of the numerical experiments we confine ourselves to a discussion of variability of the near-bottom temperature. The numerical experiments aimed at forecasting the future climatic state of the ocean were carried out using six versions of the atmospheric forcing from the CMIP5 output. In our experiments Arctic warming led to a gradual reduction and disappearance of the sea ice in the summer months and an increase of the temperature of the ocean upper layer. On the Arctic shelf, the thermal signal from the surface layer gradually penetrated into the deeper layers of the ocean.

The Atlantic waters entering through the Fram Strait and the Barents Sea have been always considered as one of the main sources of heat for the Arctic basin [33]. According to the observations, the variability of the atmospheric dynamics determines the intensity of the Atlantic water inflow into the Arctic basin [34]. When analyzing the spatial-temporal variability of the temperature fields, we have found that from the 2030s the ocean model simulates warming of the intermediate layer of the Arctic Ocean. This process is caused by the arrival of anomalously warm Atlantic water through the Fram Strait and the Barents Sea. The results of our experiments show that the features of the atmospheric circulation of the climatic models selected as surface forcing for the ocean model determine the spatial distribution and intensity of heat fluxes entering the Arctic basin with the ocean currents.

The model simulates warming in the near-bottom layer of the Barents and Kara Seas, as well as on the continental slope in all six experiments for all versions of the atmospheric forcing. The intensity of warming depends on the forcing used and varies from 2 to 6 degrees. The results of the simulation using the CNRM-CM5 and GFDL-CM3 models atmospheric data differ markedly (Figure 2). In the experiment with the CNRM-CM5 forcing the increase in the bottom temperature in the central part of the Arctic basin significantly exceeds the temperature in the Barents Sea. This indicates a more intensive Fram Strait branch of the Atlantic waters. On the contrary, the use of atmospheric data of the GFDL-CM3 model does not form a temperature increase along the Atlantic water passing through the Fram Strait. The bulk of the Atlantic water enters the Arctic through the Barents Sea. It is interesting to note that in the seas of the Siberian shelf there is no increase in the near-bottom temperature. The exception is the simulation using the GFDL-CM3 atmospheric data (warming up to 4 degrees in the East Siberian Sea).

A discussion of the features of the atmospheric dynamics above the Arctic Ocean in the CMIP models is not the objective of this study. We used various versions of atmospheric forcing to identify areas of the Arctic Ocean where a significant increase of the near-bottom temperature is possible. Calculation of the thermodynamic conditions for a possible existence of gas hydrates was carried out in the upper 1000-meter layer of the bottom sediments of the Arctic Ocean. In this case, the submarine permafrost-related methane hydrates are not taken into account. A previous study [14] has shown that permafrost-related gas hydrates respond very slowly to changes in the bottom water temperature for the RCP 8.5 scenario and the hydrates will remain stable for the next 100 years.

The simulated hydrate stability zone for 2006 is shown in Figure 3. The pressure-temperature conditions are suitable for the methane hydrate accumulations beginning with ocean water depths of 250-300 meters. It should be noted that here we do not consider deep-sea areas of the Arctic Ocean (water depths exceeding 3000 m), since they are not considered to be gas-bearing. The lower boundary of the GHSZ depth in the bottom sediment column can reach 1000 m due to a low geothermal flow and large water depth, as was found in the Canada Basin (Figure 3). The sea bottom is not always the upper boundary of the GHSZ, and, thus, at water depths lower than 300 m this boundary lies at a depth of about 50 m below the bottom.

It should be emphasized that favorable pressure-temperature conditions are not sufficient for the existence of gas hydrate deposits. To accumulate a gas hydrate, it is necessary that the methane content exceed the limit of its solubility in water. The shelf area, where there is an increased content of methane in the bottom sediments, is of great interest. Such areas have been identified in the Barents Sea. It is believed that the increased methane content in these areas is the consequence of upward migration of the gas through faults [35]. According to our estimates, the GHSZ thickness on the Barents Sea shelf can reach not more than 200 m, since the Barents Sea is characterized by shallow bathymetry.

The sensitivity of the GHSZ to the ocean bottom temperature variations during the 21st century was estimated by employing the SibCIOM ocean model with atmosphere forcing by an ensemble of six CMIP5 climate models under the RCP8.5 scenario. Figure 4 shows the predicted shift of the GHSZ upper boundary or the complete destruction of the hydrate inventories for 2006-2100. According to the results obtained, the methane hydrates that are present in sediments at sea depths of 250-500 m are most affected by the ocean bottom water warming (Figure 4).

The warm North Atlantic Water will have a major influence on the state of the Arctic gas hydrates. The greatest relative changes in the methane hydrate stability will occur in the Barents Sea region, near the Norwegian Continental margin. According to our estimates, an increase in the bottom water temperature in these areas have brought about a vertical reduction in the GHSZ thickness by 10-40 m in 1990-2006, and over the next 100 years it may lead to a further shift of the stability zone upper boundary by 10-110 m (Figure 4). The methane hydrates in the Barents Sea region, at the Norwegian continental margin, the West Svalbard continental margin, and on the Eurasian continental shelf are most susceptible to destabilization in calculations with the whole atmospheric forcing.

Downward shift of the upper boundary of the GHSZ and a possible degradation of methane hydrates can lead to the accumulation of free methane in the layers of bottom sediments. Observations of large emissions reported in papers [7, 8, 9] are consistent with the estimates obtained in this study. The main difference of the marine hydrates from the previously considered permafrost-related hydrates [13, 12, 16] is that they can exist at small bottom depths and even near the bottom. Therefore, they are less resistant to the ongoing processes of warming in the near-bottom layer of water.

4. Conclusions

The sensitivity of the methane hydrates stability zone to the ocean bottom temperature variations during the 21st century was assessed by the regional SibCIOM model with an atmosphere forcing produced by an ensemble of six CMIP5 climate models with the RCP8.5 scenario. According to the results of the calculations, the shallow and mid-depth regions containing methane hydrates at sea depths of 250-500 m are most susceptible to the warming effects. Anomalously warm North Atlantic water entering the Arctic Ocean through the Fram Strait and the Barents Sea simulated by the SibCIOM will have a major influence on the warming of the near-bottom waters and, hence, on the Arctic gas hydrates.

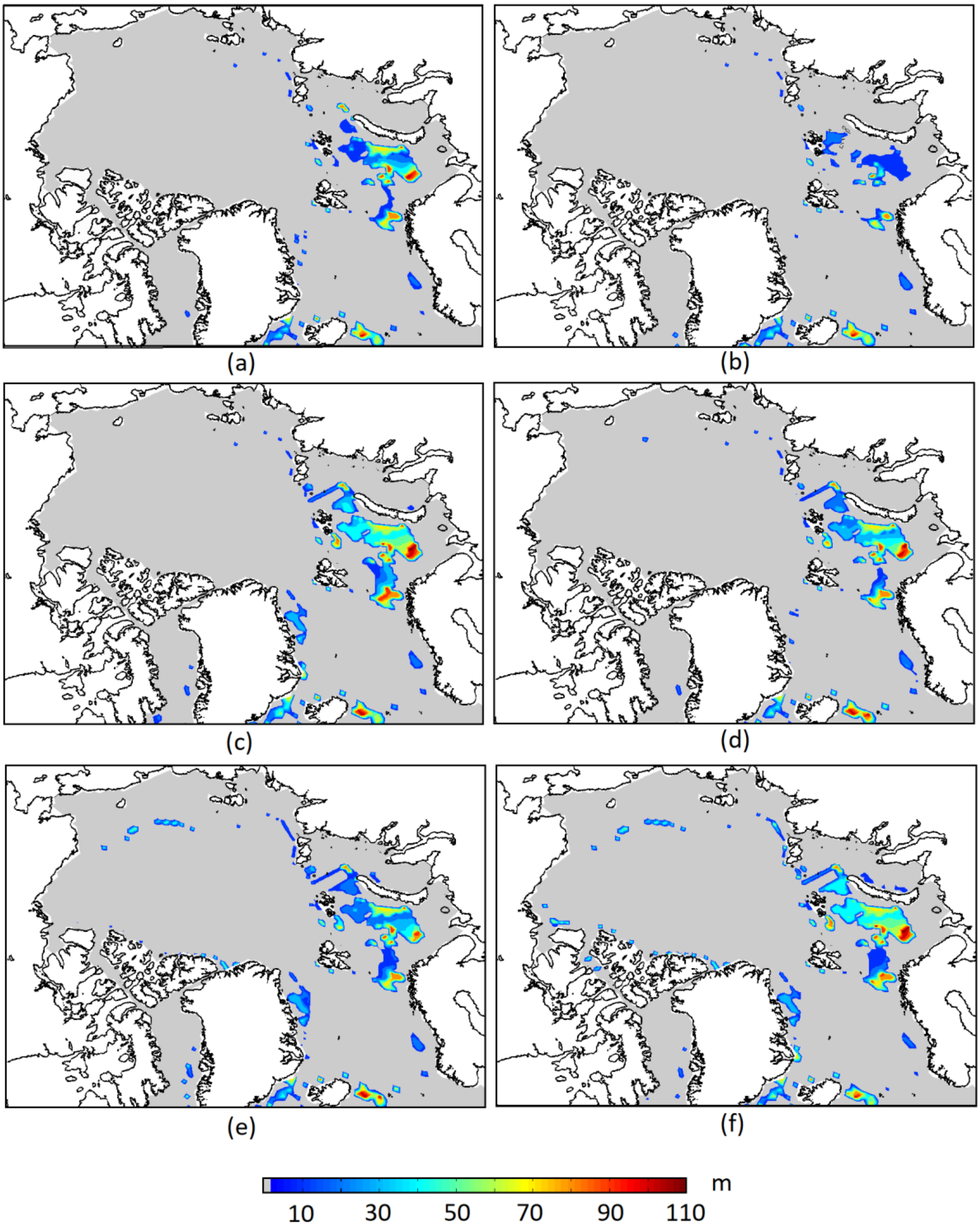

Figure 4. Change of the depth of the upper boundary of the gas hydrate stability zone (value for year 2100 minus value for year 2006) obtained in numerical experiments with atmospheric forcing from the

RCP 8.5 simulations with (a) INM-CM4, (b) BCC-CSM-1.1, (c) IPSL-CM5B-LR, (d) MPI-ESM-LR, (e) CNRM-CM5, (f) GFDL-CM3.

The areas where hydrates are most susceptible to the destruction during the next 100 years are least sensitive to the choice of a climate model. In such regions as the Barents Sea, the West Svalbard continental margin, and the continental shelf of Norway, methane hydrates may exist in shallow waters where the strongest warming occurs. For this reason, these regions are most sensitive to releasing methane into the ocean and the atmosphere when the seawater temperature is increased by approximately 2-3 °C. According to our estimates, the seafloor water warming in these areas during the next 100 years may lead to a shift in the upper boundary of the stability zone by 10-110 m.

Acknowledgments
This work was supported by the Russian Foundation for Basic Research (grants no. 17-05-00396, 17-05-00382, 18-05-00087, and 18-05-60111), the Ministry of Education and Science of the Russian Federation (grant no. 14.616.21.0082). The ocean temperature analysis was carried out under ICMMG SB RAS budget project 0315-2018-0016.

References

[1] Ruppel C D and Kessler J D 2017 The interaction of climate change and methane hydrates *Reviews of Geophysics* 55 126-68
[2] James R H *et al* 2016 Effects of climate change on methane emissions from seafloor sediments in the Arctic Ocean: A review *Limnology and Oceanography* **61** (S1) S283-S299
[3] Biastoch A, Treude T, Rupke L H 2011 Rising Arctic Ocean temperatures cause gas hydrate destabilization and ocean acidification *Geophysical Research Letters* **38** (8) L08602
[4] Kretschmer K, Biastoch A, Rupke L, Burwicz E 2015 Modeling the fate of methane hydrates under global warming *Glob. Biogeochem Cycles* **29** (5) 610–25
[5] Turner J, Overland J 2009 Contrasting climate change in the two polar regions Polar Research 28 (2) 146-64
[6] IPCC, 2013. Summary for Policymakers in Climate Change 2013: The Physical Science Basis ed Stocker T F *et al* (Cambridge University Press, Cambridge, UK and New York, NY, USA) 3–29
[7] Yurganov L N, Leifer I, Lund Myhre C 2016 Seasonal and interannual variability of atmospheric methane over Arctic Ocean from satellite data *Current problems in remote sensing of the Earth from space* **13** (2) 107-19
[8] Westbrook G et al 2009 Escape of methane gas from the seabed along the West Spitsbergen continental margin *Geophys. Res. Lett.* **36** L15608
[9] Berndt C, Feseker T, Treude T, Krastel S, Liebetrau V, Niemann H, Bertics V, Dumke I, Dünnbier K, Ferré, B, Graves C, Gross F, Hissmann K, Hühnerbach V, Krause S, Lieser K, Schauer J, Steinle L 2014 Temporal constraints on hydrate–controlled methane seepage off Svalbard *Science* **343** 284–87
[10] Portnov A, Mienert J, Serov P 2014 Modeling the evolution of climate sensitive Arctic subsea permafrost in regions of extensive gas expulsion at the West Yamal shelf *J. Geophys. Res.: Biogeosciences* **119** (11) 2082-94
[11] Shakhova N, Semiletov I, Leifer I, Sergienko V, Salyuk A, Kosmach D, Chernykh D, Stubbs C, Nicolsky D, Tumskoy V, Gustafsson O 2014 Ebullition and storm-induced methane release from the East Siberian Arctic Shelf *Nature Geoscience* **7** 64–70
[12] Romanovskii N N, Hubberten H W, Gavrilov A V,Eliseeva A A , Tipenko G S 2005 Offshore permafrost and gas hydrate stability zone on the shelf of East Siberian Seas *Geo-Mar. Lett.* **25** 167–82

[13] Malakhova V V, Eliseev A V 2017 The role of heat transfer time scale in the evolution of the subsea permafrost and associated methane hydrates stability zone during glacial cycles *Glob. Planet. Change* **157** 18-25
[14] Eliseev A, Malakhova V, Arzhanov M, Golubeva E, Denisov S, and Mokhov I 2015 Changes in the boundaries of the permafrost layer and the methane hydrate stability zone on the Eurasian Arctic Shelf, 1950–2100 *Doklady Earth Sciences* **465** (2) 1283–88
[15] Anisimov O O, Zaboikina Y Y, Kokorev V V, Yurganov L L 2014 Possible causes of methane release from the East Arctic seas shelf *Ice and Snow* **54** (2) 69–81
[16] Malakhova V V, Eliseev A V 2018 Influence of rift zones and thermokarst lakes on the formation of subaqueous permafrost and the stability zone of methane hydrates of the Laptev sea shelf in the Pleistocene *Ice and Snow* **58** (2) 231-42
[17] Malakhova V V, Golubeva E N, Iakshina D F 2017 Sensitivity of the Arctic Ocean gas hydrate to climate changes in the period of 1948-2015 *Proc. SPIE: 23rd International Symposium on Atmospheric and Ocean Optics: Atmospheric Physics* **10466** 1046656
[18] Golubeva E N, Platov G A 2007 On improving the simulation of Atlantic Water circulation in the Arctic Ocean *J Geophys. Res.* **112** C04S05
[19] Golubeva E N, Platov G A 2009 Numerical Modeling of the Arctic Ocean Ice System Response to Variations in the Atmospheric Circulation from 1948 to 2007 *Izvestiya, Atmospheric and Oceanic Physics* **45** (1) 137–51
[20] Moridis G J 2003 Numerical studies of gas production from methane hydrates *Society of Petroleum Engineers Journal* **32** (8) 359-70
[21] Kalnay E et al 1996 The NCEP/NCAR 40-Year Reanalysis Project. Bulletin of the American Meteorological Society 77 437- 71
http:www.esrl.noaa.gov/psddata/reanalysis/reanalysis.shtml, last access: 2 April 2015
[22] Taylor K E, Stouffer R J, and Meehl G A 2012 An Overview of CMIP5 and the Experiment Design *Bulletin of the American Meteorological Society* **93** 485-98
[23] Leonard B P, Lock A P, MacVean M K 1996 Conservative explicit unrestricted-timestep multidimensional constancy-preserving advection schemes *Mon. Wea. Rev.* **124** 2588–606
[24] Golubeva E N, Ivanov Ju A, Kuzin V I, Platov G A 1992 Numerical modeling of the World Ocean circulation including upper ocean mixed layer *Oceanology* **32** (3) 395-405
[25] Hunke E C, Dukowicz J K 1997 An elastic-viscous-plastic model for ice dynamics *J. Phys. Oceanography* **27** (9) 1849–67
[26] Bitz C M, Lipscomb W H 1999 An energy-conserving thermodynamic model of sea ice *J. Geophys. Res.* **104** (C7) 15669-77
[27] Lipscomb W H, Hunke E C 2004 Modeling Sea Ice Transport Using Incremental Remapping *Mon. Wea. Rev.* **132** (6) 1341–54
[28] Steele M, Morley R, Ermold W 2001 PHC: A global hydrography with a high quality Arctic Ocean *J. Climate* **14** (9) 2079–87
[29] Pithan F, Mauritsen T 2014 Arctic amplification dominated by temperature feedbacks in contemporary climate models *Nature Geoscience* **7** 181-4
[30] Hunter S, Goldobin D, Haywood A, Ridgwell A, Rees J 2013 Sensitivity of the global submarine hydrate inventory to scenarios of future climate change *Earth and Planetary Science Letters* **367** 105–15
[31] Davies J H 2013 Global map of Solid Earth surface heat flow *Geochem. Geophyst. Geosyst.* **14** 4608-22
[32] Marín-MorenoH, Minshull T, Westbrook G, and Sinha B 2015 Estimates of future warming-induced methane emissions from hydrate offshore west Svalbard for a range of climate models *Geochem. Geophys. Geosyst.* **16** 1307–23
[33] Rudels B, Korhonen M, Schauer U, Pisarev S, Rabe B, Wisotzki A 2015 Circulation and transformation of Atlantic water in the Eurasian Basin and the contribution of the Fram Strait inflow branch to the Arctic Ocean heat budget *Prog. Oceanogr.* **132** 128–52

[34] Karcher M, Smith J N, Kauker F, Gerdes R, Smethie W M 2012, Recent changes in Arctic Ocean circulation revealed by iodine-129 observations and modeling *J. Geophys. Res.* **117** C08007 doi:10.1029/2011JC007513

[35] Archegov V B 2015 Thermobaric conditions of base gas-hydrates formation and risk of their destruction at development of the shtokman gas-condensate field *Proceedings of the Komi Science Centre of the Ural Branch of the Russian Academy of Sciences* **2** (22) 65-70